



Multiple lump solutions and their interactions for an integrable nonlinear dispersionless PDE in vector fields

Tahira Batool^a, Aly R. Seadawy^{b,1} , Syed T.R. Rizvi^a

^aDepartment of Mathematics, COMSATS University Islamabad, Lahore Campus, Pakistan

^bMathematics Department, Faculty of Science, Taibah University, Al-Madinah Al-Munawarah, Saudi Arabia
aabdelalim@taibahu.edu.sa

Received: April 11, 2022 / **Revised:** January 14, 2023 / **Published online:** February 22, 2023

Abstract. In this article, lump solutions, lump with I-kink, lump with II- kink, periodic, multiwaves, rogue waves and several other interactions such as lump interaction with II-kink, interaction between lump, lump with I-kink and periodic, interaction between lump, lump with II-kink and periodic are derived for Pavlov equation by using appropriate transformations. Additionally, we also present 3-dimensional, 2-dimensional and contour graphs for our solutions.

Keywords: Pavlov equation, lump and multiwaves, rogue waves, ansatz transformations.

1 Introduction

Nonlinear evolution equations (NLEEs) are significantly used to observe numerous physical phenomena that appear in mathematical physics, condensed matter physics, water surface gravity waves, ion-acoustic waves in plasmas etc. [7, 9, 27, 29, 30, 36]. The exact solutions for NLEEs play a vital role to study the dynamics of the evolution of native phenomena. There are so many nonlinear integrable models in various fields of sciences that consist of so many types of soliton solutions like bright and singular dromions, domain walls, complexitons, positons and lump solitons [2]. Since for the discovery of solitons, so many integration strategies like inverse scattering transformation [1], Hirota bilinear approach (HBA) [24], fractional Riccati method [32], tanh-coth approach [11], homogeneous balance approach, Jacobi elliptic function technique [10], Darboux transformation [35], the (G'/G) expansion architectonic [31] and many other have been developed to study various nonlinear models arising in distinct areas of sciences like optical fiber, plasmas physics, fluid mechanics, biology etc.

Solitons play a pivotal role in studying the integrable system. In the community of mathematical physics, the various solutions such as lump solutions have gathered

¹Corresponding author.

considerable attention in current years. Lump solutions are primarily rational function solutions confined in all possible directions in the space. Same as solitons, they have several major applications in nonlinear dynamics. For instance, they could be applied to express nonlinear figured in plasma and nonlinear optic media etc. Over the ages, lump solutions have been set up and discussed for numerous integrable equations, for instance, Kadomtsev–Petviashvili equation [23], the B-Kadomtsev–Petviashvili equation (BKP) [37] and the Ishimori-II equation [14].

In mathematics, a wave train or a periodic travelling wave defined as a periodic function of one dimensional space that moves with constant speed. In consequence, it is a particular class of spatiotemporal oscillation that is specifically a periodic function of time as well as space. Periodic waves contribute a vital role in various mathematical equations together with excitable systems, self-oscillatory systems and reaction diffusion advection system. Rogue waves, familiar as freak waves, episodic waves, monster waves, killer waves, abnormal waves and extreme waves are generally huge unpredictable and instantly emerging surface waves. In general, rogue waves, known also as oceanic phenomena, have come to play a vital role in comprehension of observational nature of various phenomena. Rogue waves give extensive understanding of an unexposed phenomenon. Many researchers have shown significant contributions in the interactions between lump, periodic, multi solitons and rogue wave [34]. Guo et al. found lump solutions, lump with one-strip solution and observed their interactions with the different combinations of exponential functions of dimensionally reduced NLEEs [13]. In [17], Liu worked on lump soliton solutions and their interactions with the double exponential function and lump with two kink for Korteweg–De Vries equation (KdV). In [4], Ahmed et al. analyzed M -shaped rational solitons and the interactions with kink solution waves. In [3], Ahmed et al. worked on monoclinic breather solution and found interactional phenomena with the multikink waves and multiwave for an NLEE. Ma established Riemann–Hilbert problems and presenting soliton solutions for nonlocal reverse-time nonlinear Schrödinger hierarchies associated with higher-order matrix spectral problems [20]. Ma conducted two nonlocal group reductions of the AKNS matrix spectral problems to generate a class of nonlocal reverse-spacetime integrable mKdV equations [18]. Ma proposed a kind of nonlocal real reverse-spacetime integrable hierarchies of PT-symmetric matrix AKNS equations through nonlocal symmetry reductions on the potential matrix [19]. A kind of novel reduced nonlocal integrable mKdV equations of odd order was presented by taking two group reductions of the AKNS matrix spectral problems [21, 22].

We intend to obtain distinct forms of lump soliton and their interactions like lump with I-kink, lump with II-kink, periodic waves, interaction between periodic lump and kink wave, multiwave solutions and rogue wave solitons for well-defined Pavlov equation [15]. We will use ansatz transformations to obtain these lump solutions with constraint conditions

$$\Omega_{xx} = \Omega_{tx} + \Omega_y \Omega_{xx} - \Omega_x \Omega_{xy}, \quad (1)$$

where $\Omega(x, y, t)$ represents the amplitude of the related wave. Equation (1) emerge during the investigation of integrable hydrodynamic chains [8]. The above equation is a nonlinear differential equation, which is an example of integrable dispersion. The governing model

is classified among the elementary integrable systems of vector fields make an appearance from several problems of differential geometry and mathematical physics.

The content of this paper is arranged as follows. In Section 2, we find out lump solitons. In Section 3, we will investigate lump with I-kink solutions. In Section 4, we present lump with II-kink solution. In Section 5, we present periodic solutions. In Section 6, we evaluate rogue wave. In Section 7, we will evaluate multiwave solutions. In Section 8, we will study result and discussions, and in Section 9, we will present concluding remarks.

2 Lump solitons

In order to compute lump solitons for Eq. (1), we use the transformation [40]

$$\Omega = m_0 + 2\beta(\ln \rho)_x. \quad (2)$$

By using Eq. (2) into Eq. (1) we obtain the following bilinear form:

$$\begin{aligned} & 2\rho\rho_y^3 - 3\rho^2\rho_y\rho_{yy} + \rho^3\rho_{yyy} - 2\rho\rho_t\rho_y\rho_x + 2\rho\rho_t\rho_y\rho_x + \rho^2\rho_{yt}\rho_x \\ & - 2\beta\rho_y\rho_{yy}\rho_x^2 + \rho^2\rho_y\rho_{xt} + \rho^2\rho_t\rho_{xy} + 4\beta\rho_y^2\rho_x\rho_{xy} + 2\beta\rho\rho_{yy}\rho_x\rho_{xy} \\ & - 4\beta\rho\rho_y\rho_{xy}^2 - \rho^3\rho_{xyt} - 2\beta\rho\rho_y\rho_x\rho_{xyy} + 2\beta\rho^2\rho_{xy} + \rho_{xyy} - 2\beta\rho_y^3\rho_{xt} \\ & + 2\beta\rho\rho_y\rho_{yy}\rho_{xx} + 2\beta\rho\rho_y^2\rho_{xxy} - 2\beta\rho^2\rho_{yy}\rho_{xxy} = 0. \end{aligned} \quad (3)$$

Now we use Eq. (3) to formulate lump solutions with the help of the following transformation [26]:

$$\rho = \phi^2 + \psi^2 + \xi_9, \quad (4)$$

where

$$\phi^2 = \xi_1x + \xi_2y + \xi_3t + \xi_4, \quad \psi^2 = \xi_5x + \xi_6y + \xi_7t + \xi_8.$$

However, ξ_α ($1 \leq \alpha \leq 9$), are arbitrary parameters to be determined. Now, by replacing Eq. (4) into Eq. (3) relating the coefficients of x , y and t , we get the system of equations.

2.1 Set-I

Considering $\xi_1 = 0$, $\xi_4 = 0$ and $\xi_6 = 0$ and using the obtained system of equations, we get reduced system of equations. By solving reduced system of equations using Maple we determined the following parameters:

$$\xi_3 = \sqrt{-2\xi_7}, \quad \xi_5 = \frac{-3\xi_2^2}{2\xi_7}, \quad \xi_7 = \xi_7, \quad \xi_8 = \xi_8, \quad \xi_9 = \frac{-3\xi_2^4}{2\xi_7^2}.$$

We use parameters in Eq. (4), then we use (2) to produce the required solution of Eq. (1).

$$\begin{aligned} \Omega(x, y, t) = & m_0 + 4\xi_2\beta(\iota\sqrt{2\xi_7}t + \xi_2y) \\ & \times \left(\frac{-3\xi_2^4\beta}{2\xi_7^2} + \left(\xi_7t - \frac{3\xi_2^2x}{2\xi_7} \right)^2 + \iota(\sqrt{2\xi_7}t + \xi_2y)^2 \right)^{-1}, \end{aligned} \quad (5)$$

where Ω represents the lump solution of Eq. (1).

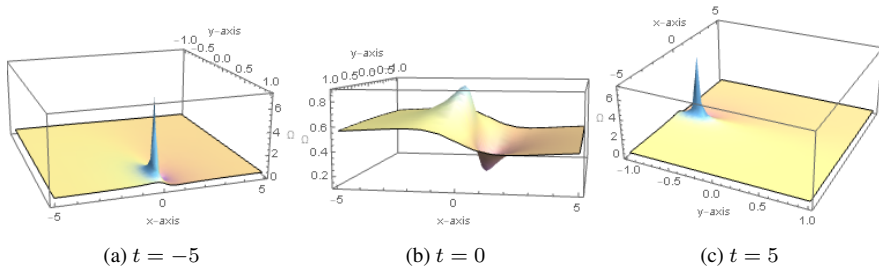


Figure 1. The 3-D graphs for $\Omega(x, y, t)$ in Eq. (5) are presented with the following values of parameters: $\xi_2 = 1, \xi_7 = -0.75, \xi_8 = 1, m_0 = 0.5, \beta = -0.1$ in interval $-5 \leq x \leq 5$ and $-1 \leq y \leq 1$.

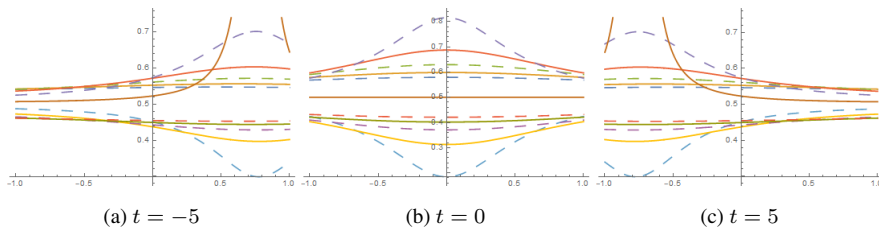


Figure 2. The 2-D graphs for the $\Omega(x, y, t)$ in Eq. (5) are shown with the following parametric values: $\xi_2 = 1, \xi_7 = -0.75, \xi_8 = 1, m_0 = 0.5, \beta = -0.1$.

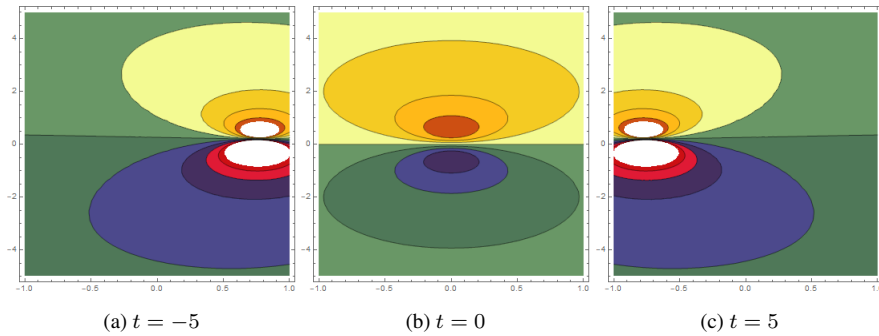


Figure 3. The contour graphs for $\Omega(x, y, t)$ in Eq. (5) are presented with the following values of parameters: $\xi_2 = 1, \xi_7 = -0.75, \xi_8 = 1, m_0 = 0.5, \beta = -0.1$ in interval $-5 \leq x \leq 5$ and $-1 \leq y \leq 1$.

2.2 Set-II

Taking $\xi_1 = 0, \xi_4 = 0$ and $\xi_6 = 0$ and using the obtained system of equations, we get the reduced system of equations. By solving reduced system of equations using Maple we found the values of parameters:

$$\xi_2 = \xi_2, \quad \xi_3 = 0, \quad \xi_5 = \frac{-3\xi_2^2 y}{4\xi_7}, \quad \xi_7 = \xi_7, \quad \xi_8 = \xi_8, \quad \xi_9 = \frac{-3\xi_2^4 \beta}{4\xi_7^2}.$$

We use the above parameters in Eq. (4), then we use Eq. (2) to reveal the required solution of Eq. (1).

$$\Omega(x, y, t) = m_0 + 4\xi_2^2\beta y \left(\frac{-3\xi_2^4\beta}{4\xi_7^2} + \left(\xi_8 + \xi_7 t - \frac{3\xi_2^2 x}{4\xi_7} \right)^2 + \xi_2^2 y^2 \right)^{-1},$$

where Ω specify the lump solution of Eq. (1).

3 Lump with I-kink

We use the bilinear form presented in Eq. (3) and the transformation [39]

$$\rho = \phi^2 + \psi^2 + \xi_9 + b_1 e^{\rho_1}, \tag{6}$$

where

$$\begin{aligned} \phi^2 &= \xi_1 x + \xi_2 y + \xi_3 t + \xi_4, & \psi^2 &= \xi_5 x + \xi_6 y + \xi_7 t + \xi_8, \\ \rho_1 &= \lambda_1 x + \lambda_y + \lambda_3 t. \end{aligned}$$

However, ξ_α ($1 \leq \alpha \leq 9$), λ_1 , λ_2 and λ_3 all are specific parameters to be calculated. By substituting Eq. (6) into Eq. (3) and resolving the coefficients of x , y , t and exponential term, we found the system of equations.

3.1 Set-I

We consider $\xi_3 = \xi_6 = \xi_8 = 0$. Using the obtained system of equations, we get the reduced system of equations. By solving reduced system of equations using Maple we get the values of parameters:

$$\begin{aligned} \xi_1 &= \xi_1, & \xi_2 &= \xi_2, & \xi_4 &= \frac{-1}{2}\xi_2\sqrt{2}\sqrt{3}, & \xi_5 &= \xi_5, & \xi_7 &= \xi_7, & \xi_9 &= \xi_9, \\ \lambda_1 &= \frac{\sqrt{\frac{-1}{6}(-4b\xi_5^2 - 45\xi_2^2b)}}{\xi_2}, & \lambda_2 &= \frac{1}{3}\sqrt{2}\sqrt{3}, \\ \lambda_3 &= \frac{\xi_2}{\sqrt{\frac{-1}{6}(-4b\xi_5^2 - 45\xi_2^2b)}}. \end{aligned}$$

By substituting the above parameters into Eq. (6), then using Eq. (2) we find the required lump with I-kink solution for Eq. (1)

$$\begin{aligned} \Omega(x, y, t) &= m_0 + 2\beta \left(\sqrt{\frac{2}{3}}\mathfrak{A}b_1 + 2\xi_2 \left(\xi_1 x + 2\xi_2 \left(\xi_1 x + \xi_2 \left(-\sqrt{\frac{3}{2}} + y \right) \right) \right) \right) \\ &\times \left(\xi_9 + \mathfrak{A}b_1 + (\xi_7 t + \xi_5 x)^2 + \left(\xi_1 x + \xi_2 \left(-\sqrt{\frac{3}{2}} + y \right) \right)^2 \right)^{-1}, \tag{7} \end{aligned}$$

where $\mathfrak{A} = \exp\{6\xi_2 t / \sqrt{45\xi_2^2/\beta + 4\xi_5^2} + \sqrt{45\xi_2^2/\beta + 4\xi_5^2}x/\xi_2 + 2y\}$.

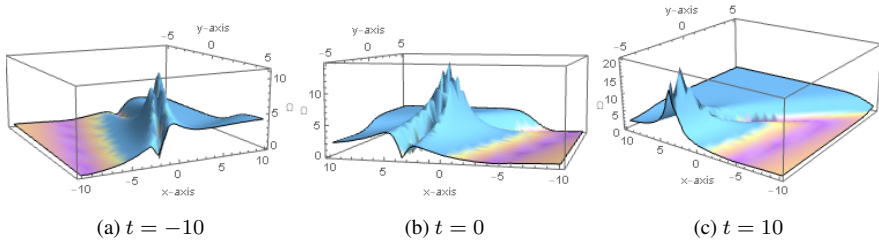


Figure 4. The 3-D graphs for $\Omega(x, y, t)$ in Eq. (7) are presented with the following values of parameters: $\xi_1 = 10, \xi_2 = 20, \xi_5 = 5, \xi_7 = 2, \xi_9 = 2, m_0 = 1, \beta = 2, b_1 = 22$ in interval $-10 \leq x \leq 10$ and $-5 \leq y \leq 5$.

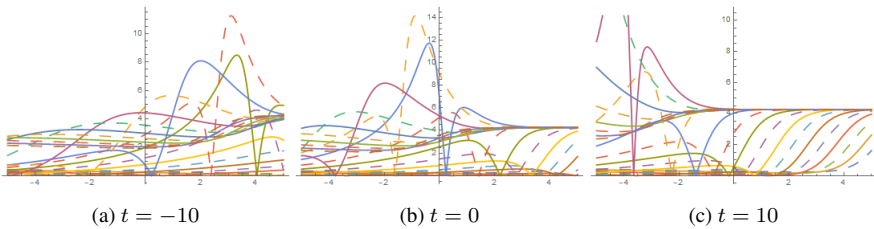


Figure 5. The 2-D graphs for $\Omega(x, y, t)$ in Eq. (7) are presented with the following parametric values: $\xi_1 = 10, \xi_2 = 20, \xi_5 = 5, \xi_7 = 2, \xi_9 = 2, m_0 = 1, \beta = 2, b_1 = 22$.

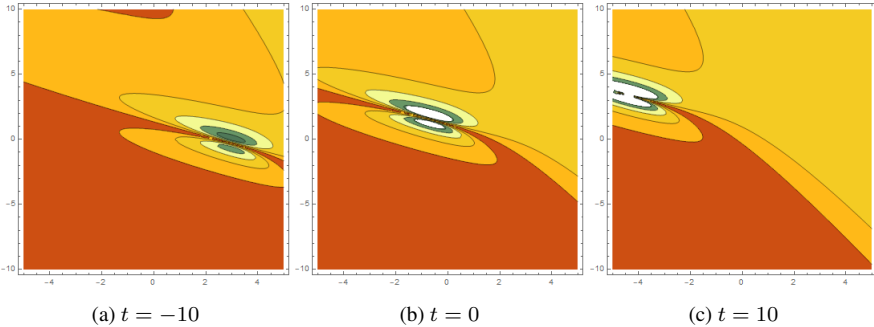


Figure 6. The contour graphs for $\Omega(x, y, t)$ in Eq. (7) are presented with the following values of parameters: $\xi_1 = 10, \xi_2 = 20, \xi_5 = 5, \xi_7 = 2, \xi_9 = 2, m_0 = 1, \beta = 2, b_1 = 22$ in interval $-10 \leq x \leq 10$ and $-5 \leq y \leq 5$.

3.2 Set-II

We take $\xi_3 = \xi_6 = \xi_8 = 0$. Using the obtained system of equations, we get reduced system of equations. By solving reduced system of equations using Maple we get the values of parameters:

$$\begin{aligned} \xi_1 = \xi_1, \quad \xi_4 = \xi_4, \quad \xi_5 = \xi_5, \quad \xi_7 = \xi_7, \quad \xi_9 = \xi_9, \quad \lambda_1 = \lambda_1, \\ \lambda_2 = \frac{\sqrt{-9\beta\lambda_1^2\xi_4^2 + 9\beta\xi_5^2 + 81\xi_4^2\xi_4}}{\beta\lambda_1^2\xi_4^2 - \beta\xi_5^2 - 3\xi_4^2}, \quad \lambda_3 = \frac{-3(\beta\lambda_1^2 + \xi_4^2 - \beta\xi_5^2 - 9\xi_4^2)}{\lambda_1(\beta\lambda_1^2 + \xi_4^2 - \beta\xi_5^2 - 3\xi_4^2)}, \\ \xi_2 = \frac{\sqrt{-9\beta\lambda_1^2\xi_4^2 + 9\beta\xi_5^2 + 81\xi_4^2\xi_4}}{\beta\lambda_1^2\xi_4^2 - \beta\xi_5^2 - 3\xi_4^2}. \end{aligned}$$

Using the above parameters into Eq. (6) and using Eq. (2), we get the required lump with I-kink solution for Eq. (1).

$$\begin{aligned} \Omega(x, y, t) = m_0 + 2\beta \left(3\mathfrak{B} + 3\lambda_1\xi_4\sqrt{(9 - \beta\lambda_1^2 + \beta\xi_5^2)b_1} \right. \\ \left. - \frac{6\xi_4^2\sqrt{(9 - \beta\lambda_1^2 + \beta\xi_5^2)b_1}}{(-3 + \beta\lambda_1^2)\xi_4^2 - \beta\xi_5^2} \left(\xi_4 + \xi_3t + \xi_1x - \frac{3\xi_4^2\sqrt{(9 - \beta\lambda_1^2)\xi_4^2 + \beta\xi_5^2y}}{(-3 + \beta\lambda_1^2)\xi_4^2 - \beta\xi_5^2} \right. \right. \\ \left. \left. + 2\xi_6(\xi_8 + \xi_7t + \xi_6y + \xi_5x) \right) \right) \\ \times \left(\xi_9 + \mathfrak{B}b_1 + \left(\xi_4 + \xi_3t + \xi_1x - \frac{3\xi_4^2\sqrt{(9 - \beta\lambda_1^2)\xi_4^2 + \beta\xi_5^2y}}{(-3 + \beta\lambda_1^2)\xi_4^2 - \beta\xi_5^2} \right)^2 \right. \\ \left. + (\xi_8 + \xi_7t + \xi_5x + \xi_6y)^2 \right)^{-1}, \end{aligned} \quad (8)$$

where $\mathfrak{B} = \exp\{(\beta\xi_5^2(3t - \lambda_1^2x)\xi_4^2 - 3(-9 + \beta\lambda_1^2)t + \lambda_1^2(-3 + \beta\lambda_1^2)x) + 3\lambda_1\xi_4\}/(\lambda_1(-3 + \beta\lambda_1^2)\xi_4^2 - \beta\xi_5^2)\}$. In Eq. (8), Ω represents the lump with I-kink solution of Eq. (1).

4 Lump with II-kink

For lump with II-kink, we use bilinear equation given in Eq. (3) along with following transformation [28]:

$$\rho = \phi^2 + \psi^2 + \xi_9 + b_1e^{\rho_1} + b_2e^{\rho_2}, \quad (9)$$

where

$$\begin{aligned} \phi^2 = \xi_1x + \xi_2y + \xi_3t + \xi_4, \quad \psi^2 = \xi_5x + \xi_6y + \xi_7t + \xi_8, \\ \rho_1 = \lambda_1x + \lambda_2y + \lambda_3t, \quad \rho_2 = \lambda_4x + \lambda_5y + \lambda_6, \end{aligned}$$

where ξ_α ($1 \leq \alpha \leq 9$) and λ_i ($1 \leq i \leq 6$) are all parameters to be found. By replacing Eq. (9) into Eq. (3) and calculating the coefficients of t , y , x and exponential terms we obtain system of equations, where Ω represents the lump with II-kink solution of Eq. (1).

4.1 Set-I

We assume $\xi_1 = \xi_4 = \xi_6 = \lambda_2 = \lambda_1 = 0$. With the aid of the above mentioned assumptions and using the obtained system of equations we get reduced system of equations. By

solving reduced system of equations using Maple we get the values of parameters:

$$\begin{aligned} \xi_2 &= \frac{\lambda_5 \xi_3 (2\lambda_4^2 \xi_7 + 3\lambda_5^2 \xi_5 - 2\xi_5)}{\lambda_4 \xi_7}, \quad \xi_3 = \xi_3, \quad \xi_5 = \xi_5, \quad \xi_7 = \xi_7, \\ \xi_9 &= \lambda_3 = \frac{-3(\lambda_5^2 - 1)}{\lambda_4}, \quad \lambda_4 = \lambda_4, \quad \lambda_5 = \lambda_5, \quad \lambda_6 = \frac{1}{\lambda_4}, \\ \xi_8 &= (12\lambda_4^4 \lambda_5^2 \xi_3^2 \xi_7^2 + 36\lambda_4^2 \lambda_5^4 \xi_3^2 \xi_5 \xi_7 + 27\lambda_5^6 \xi_3^2 \xi_5^2 - 24\lambda_4^2 \lambda_5^2 \xi_3^2 \xi_5 \xi_7 \\ &\quad - 36\lambda_5^4 \xi_3^2 \xi_5^2 + 4\lambda_4^2 \xi_3^2 \xi_5 \xi_7 + 8\lambda_4^2 \xi_5 \xi_7^3 + 12\lambda_5^2 \xi_3^2 \xi_5^2) \\ &\quad \times (36(\xi_5 \xi_7^2 \lambda_4 (\lambda_5 - 1)(\lambda_5 + 1)))^{-1}. \end{aligned}$$

We use the above parameters in Eq. (9), then in Eq. (2) to exhibit the lump with II-kink solution for Eq. (1). We get

$$\begin{aligned} \Omega(x, y, t) &= m_0 + 2\beta \left(\lambda_5 e^{t/\lambda_4 + \lambda_4 x + \lambda_5 y} b_2 \right. \\ &\quad \left. + 2 \left(\lambda_4 \lambda_5 \xi_3 + \frac{\lambda_5 (-2 + 3\lambda_5^2) \xi_3 \xi_5}{2\lambda_4 \xi_7} \right) \left(\xi_3 t + \lambda_4 \lambda_5 \xi_3 y + \frac{\lambda_5 (-2 + 3\lambda_5^2) \xi_3 \xi_5 y}{2\lambda_4 \xi_7} \right) \right) \\ &\quad \times \left(\xi_7 + e^{-3(-1 + \lambda_5^2)t/\lambda_4} b_1 + e^{t/\lambda_4 + \lambda_4 x + \lambda_5 y} b_2 + 27\lambda_5^6 \xi_3^2 \xi_5^2 \right. \\ &\quad \left. - 36\lambda_5^4 \xi_3^2 \xi_5 (\xi_5 - \lambda_4^2 \xi_7 \lambda_4 (\xi_3^2 + 2\xi_7^2 - 9\xi_7 t + \xi_5 x)) \right. \\ &\quad \left. + \frac{12\lambda_5^2 \xi_3^2 (\xi_5 - \lambda_4^2 \xi_7)^2 + 3\lambda_4 \xi_5 \xi_7^2 (\xi_7 t + \xi_5 x)^2}{1296\lambda_4^2 (-1 + \lambda_5)^2 (1 + \lambda_5)^2 \xi_5^2 \xi_7^4} \right. \\ &\quad \left. + \left(\xi_3 t + \lambda_4 \lambda_5 \xi_3 y \frac{\lambda_5 (-2 + 3\lambda_5^2) \xi_3 \xi_5 y}{2\lambda_4 \xi_7} \right) \right)^{-1}. \end{aligned} \tag{10}$$

In Eq. (10), Ω represents the lump with II-kink solution of Eq. (1).

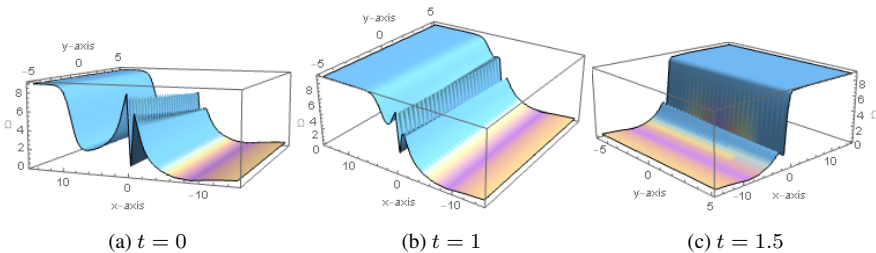


Figure 7. The 3-D graphs for $\Omega(x, y, t)$ in Eq. (10) are presented with the following values of parameters: $m_0 = 1, \lambda_5 = 2, \lambda_4 = 0.1, b_2 = 0.6, \xi_3 = 28, \xi_5 = 10, \xi_7 = 50, \beta = 2, b_1 = 4$ in interval $-10 \leq x \leq 10$ and $-5 \leq y \leq 5$.

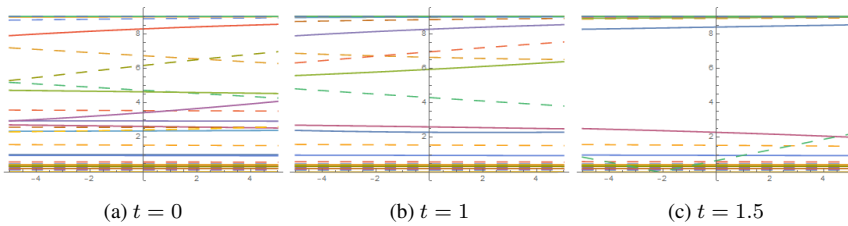


Figure 8. The 2-D graphs for $\Omega(x, y, t)$ in Eq. (10) are presented with the following parametric values: $m_0 = 1, \lambda_5 = 2, \lambda_4 = 0.1, b_2 = 0.6, \xi_3 = 28, \xi_5 = 10, \xi_7 = 50, \beta = 2, b_1 = 4$.

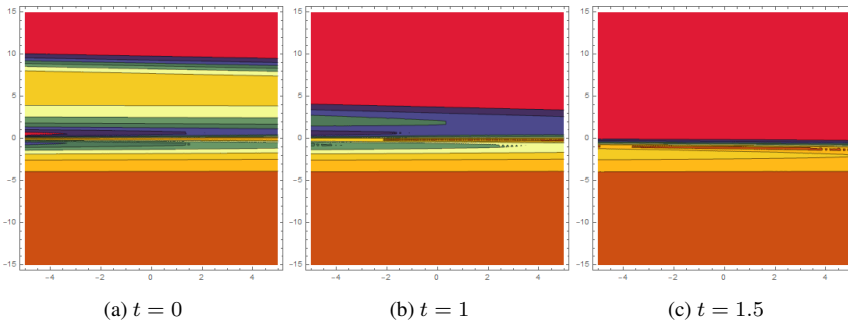


Figure 9. The contour graphs for $\Omega(x, y, t)$ in Eq. (10) are presented with the following values of parameters: $m_0 = 1, \lambda_5 = 2, \lambda_4 = 0.1, b_2 = 0.6, \xi_3 = 28, \xi_5 = 10, \xi_7 = 50, \beta = 2, b_1 = 4$ in interval $-10 \leq x \leq 10$ and $-5 \leq y \leq 5$.

4.2 Set-II

We consider $\xi_1 = \xi_4 = \xi_6 = \lambda_2 = \lambda_1 = 0$. With the help of these assumptions and using the obtained system of equations, we get reduced system of equations. By solving reduced system of equations using Maple we get the values of parameters:

$$\begin{aligned} \xi_1 = \xi_4 = \xi_6 = \lambda_2 = \lambda_1 = 0, \quad \lambda_3 &= \frac{-3\lambda_5^2}{\lambda_4}, \quad \lambda_4 = \lambda_4, \quad \lambda_5 = \lambda_5, \\ \lambda_6 &= 0, \quad \xi_2 = \xi_2, \quad \xi_3 = \xi_3, \quad \xi_5 &= \frac{-2\lambda_4^2\xi_7}{\lambda_5^2}, \\ \xi_7 = \xi_7, \quad \xi_9 = \xi_9, \quad \xi_8 &= \frac{2\lambda_4^2\xi_3^2 + 4\lambda_4^2\xi_7^2 - 9\lambda_5^2\xi_2^2}{18\xi_7\lambda_4\lambda_5^2}. \end{aligned}$$

Using the above parameters into Eq. (9) and using Eq. (2), we get the lump with II-kink solution for Eq. (1).

$$\begin{aligned} \Omega(x, y, t) &= m_0 + 2\beta\lambda_5 e^{\lambda_4 x + \lambda_5 y} b_2 \left(\xi_7 + e^{-3\lambda_5^2 t / \lambda_4} b_1 + e^{\lambda_4 x + \lambda_5 y} b_2 + \xi_3^2 t^2 \right. \\ &\quad \left. + \left(\frac{2\lambda_4^2 \xi_3^2 + 4\lambda_4^2 \xi_7^2}{18\lambda_4 \lambda_5^2 \xi_7} + \xi_7 t - \frac{2\lambda_4^2 \xi_7 x}{3\lambda_5^2} \right)^2 \right)^{-1}, \end{aligned}$$

where Ω represents the lump with II-kink solution of Eq. (1).

5 Rouge waves

For rouge wave solution, we use bilinear form presented in Eq. (3) using the transformation [38],

$$\rho = \phi^2 + \psi^2 + \xi_9 + \cosh(\lambda_1 x + \lambda_2 y + \lambda_3 t + \lambda_4) \tag{11}$$

with

$$\phi^2 = \xi_1 x + \xi_2 y + \xi_3 t + \xi_4, \quad \psi^2 = \xi_5 x + \xi_6 y + \xi_7 t + \xi_8,$$

where ξ_α ($1 \leq \alpha \leq 9$) and λ_α ($1 \leq \alpha \leq 4$) are all real parameters, which we will examine. Now substituting Eq. (6) into Eq. (3) and computing the coefficients of x, y, t and trigonometric functions, we get system of equations. After resolving we obtain values of unknown parameters.

5.1 Set-I

We have taken $\xi_2 = \xi_8 = 0$. Using the supposed values, we calculate remaining unknown parameters:

$$\begin{aligned} \lambda_1 &= \sqrt{\frac{-3}{2\beta}}, \quad \lambda_2 = \frac{\sqrt{2}\sqrt{3}}{2}, \quad \lambda_3 = \frac{-2}{3}\beta\sqrt{\frac{-3}{2\beta}}, \quad \lambda_4 = \lambda_4, \\ \xi_1 &= \xi_1, \quad \xi_3 = \sqrt{-3}\xi_7, \quad \xi_4 = \xi_4, \\ \xi_5 &= \xi_5, \quad \xi_6 = \xi_6, \quad \xi_7 = \xi_7, \\ \xi_9 &= \frac{2}{3}\beta\xi_5\xi_6\sqrt{2}\sqrt{3}\sqrt{\frac{-3}{2\beta}} - 4\xi_6\xi_7\sqrt{2}\sqrt{3}\sqrt{\frac{-3}{2\beta}} - 4\xi_4^2 - 10\xi_5\xi_7 + 6\xi_6^2. \end{aligned}$$

Using the above parameters in Eq. (11), then using Eq. (2) to reveal the solution of rogue wave for Eq. (1), we get

$$\begin{aligned} \Omega(x, y, t) &= m_0 + 2\beta \left(2\xi_6(\xi_7 t + \xi_5 x + \xi_6 y) \right. \\ &\quad \left. + \sqrt{\frac{2}{3}} \sinh \left(\lambda_4 + \frac{\frac{2t}{\sqrt{-1/\beta}} + 3\sqrt{-1/\beta}x + 2y}{\sqrt{6}} \right) \right) \\ &\quad \times \left(-\xi_4^2 + 2\sqrt{\frac{-1}{\beta}}\beta\xi_5\xi_6 + \xi_6^2 - 10\xi_5\xi_7 \right. \\ &\quad \left. - 12\sqrt{\frac{-1}{\beta}}\xi_6\xi_7 + (\xi_4 + \iota\sqrt{3}\xi_7 t)^2 + (\xi_7 t + \xi_5 x + \xi_6 y)^2 \right. \\ &\quad \left. + \cosh \left(\lambda_4 + \frac{\frac{2t}{\sqrt{-1/\beta}} + 3\sqrt{-1/\beta}x + 2y}{\sqrt{6}} \right) \right)^{-1}, \tag{12} \end{aligned}$$

where Ω represents the rogue wave solution of Eq. (1).

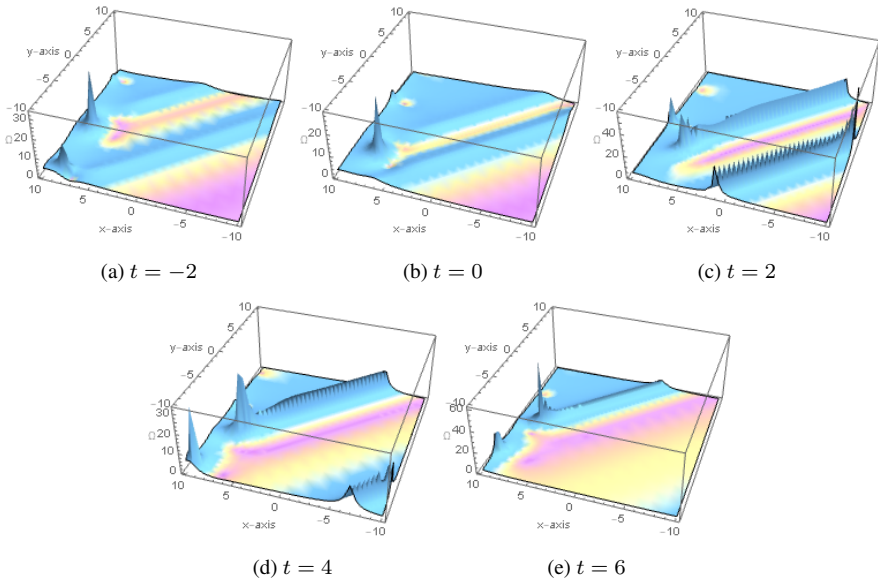


Figure 10. The 3-D plots for $\Omega(x, y, t)$ in Eq. (12) are presented with the following values of parameters: $\lambda_4 = 2, \xi_4 = 8, \xi_5 = 10, \xi_7 = 15, \xi_6 = 10, m_0 = 0.5, \beta = 2$.

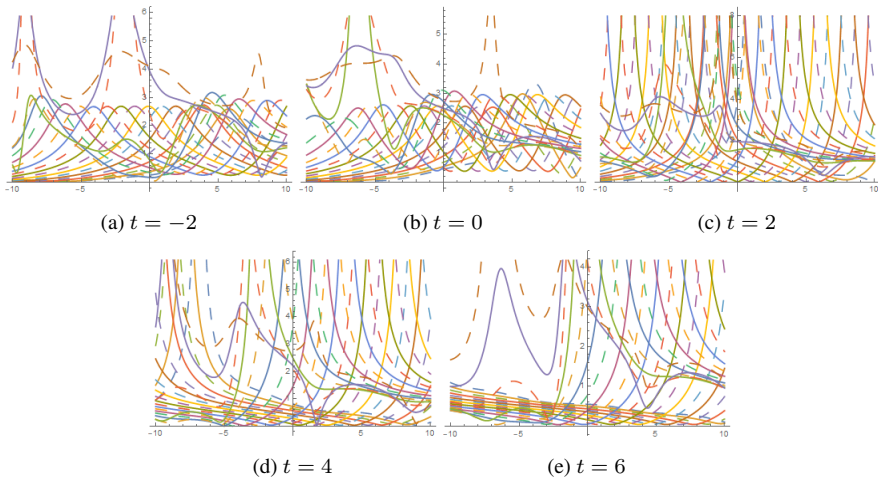


Figure 11. The 2-D plots for $\Omega(x, y, t)$ in Eq. (12) are presented with the following parametric values: $\lambda_4 = 2, \xi_4 = 8, \xi_5 = 10, \xi_7 = 15, \xi_6 = 10, m_0 = 0.5, \beta = 2$.

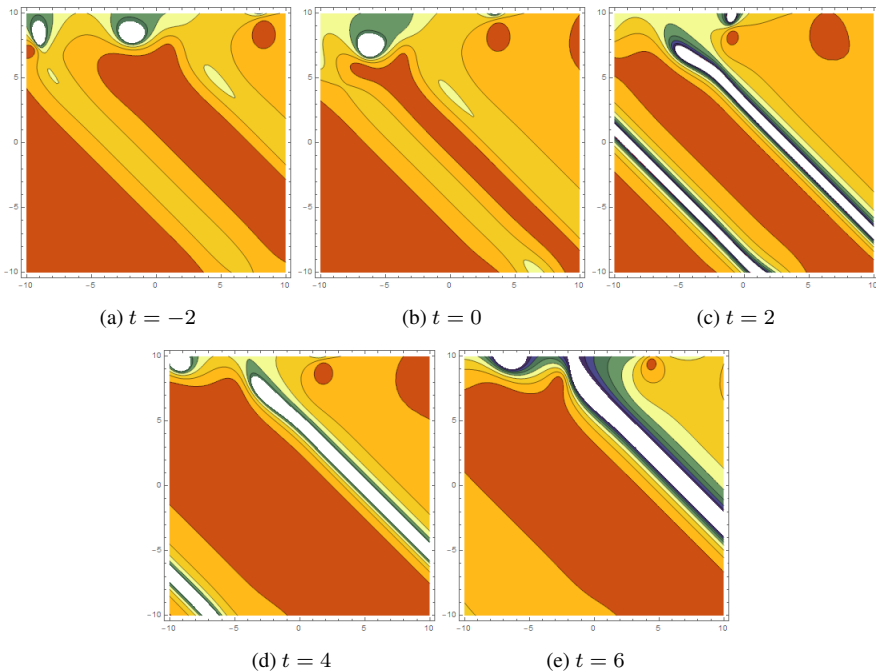


Figure 12. The contour plots for $\Omega(x, y, t)$ in Eq. (12) are presented with the following values of parameters: $\lambda_4 = 2, \xi_4 = 8, \xi_5 = 10, \xi_7 = 15, \xi_6 = 10, m_0 = 0.5, \beta = 2$.

5.2 Set-II

We have chosen $\xi_2 = \xi_8 = 0$. Now by using assumed values we find unknown parameters:

$$\begin{aligned} \xi_2 = 0, \quad \xi_8 = 0, \quad \lambda_1 &= \sqrt{\frac{-1}{\beta}}, \quad \lambda_2 = 1, \quad \lambda_3 = -\beta\sqrt{\frac{-1}{\beta}}, \\ \lambda_4 &= \lambda_4, \quad \xi_7 = \xi_7, \quad \xi_1 = \xi_1, \quad \xi_3 = \xi_3, \quad \xi_4 = \xi_4, \\ \xi_5 &= \frac{-(\xi_3^4 + 2\xi_3^2\xi_7^2 - 3\xi_7^4)}{\beta\xi_7(\xi_3^2 + 18\xi_7^2)}, \quad \xi_9 = \xi_9, \quad \xi_6 = \frac{\sqrt{\frac{-1}{\beta}}(\xi_3^2 + 3\xi_7^2)}{3\xi_7}. \end{aligned}$$

Using the above mentioned parameters in Eq. (11), then using Eq. (2) to give the solution of rogue wave for Eq. (1), we get

$$\begin{aligned} \Omega(x, y, t) &= m_0 + 2\beta \left(2\sqrt{\frac{-1}{\beta}}(\xi_3^2 + 3\xi_7^2) \left(\xi_7 t + \frac{(-\xi_3^4 - 2\xi_3^2\xi_7^2 + 3\xi_7^4)x}{\beta\xi_7(\xi_3^2 + 18\xi_7^2)} \right. \right. \\ &\quad \left. \left. + \frac{\sqrt{\frac{-1}{\beta}}(\xi_3^2 + 3\xi_7^2)y}{3\xi_7} \right) + \sinh \left(\lambda_4 - \sqrt{\frac{-1}{\beta}}bt + \sqrt{\frac{-1}{\beta}}x + y \right) \right) \end{aligned}$$

$$\times \left(\xi_9 + (\xi_4 + \xi_3 t + \xi_1 x)^2 + \left(\xi_7 t + \frac{(-\xi_3^4 - 2\xi_3^2 \xi_7^2 + 3\xi_7^4)x}{\beta \xi_7 (\xi_3^2 + 18\xi_7^2)} + \frac{\sqrt{\frac{-1}{\beta}} (\xi_3^2 + 3\xi_7^2) y}{3\xi_7} \right)^2 + \cosh \left(\lambda_4 - \sqrt{\frac{-1}{\beta}} \beta t + \sqrt{\frac{-1}{\beta}} x + y \right) \right)^{-1},$$

where Ω specify the rogue wave solution of Eq. (1).

6 Periodic waves

To find periodic wave solutions, we use the following transformation [28]:

$$\rho = \phi^2 + \psi^2 + \xi_9 + n_0 \cos(\lambda_1 x + \lambda_2 y + \lambda_3 t) \tag{13}$$

with

$$\phi^2 = \xi_1 x + \xi_2 y + \xi_3 t + \xi_4, \quad \psi^2 = \xi_5 x + \xi_6 y + \xi_7 t + \xi_8,$$

where ξ_α ($1 \leq \alpha \leq 9$), λ_α ($1 \leq \alpha \leq 3$) all are specific parameters to be examined. Substituting Eq. (13) into Eq. (3) and collecting the powers of t, x, y and trigonometric functions, we get the system of equations.

6.1 Set-I

We assume $\xi_1 = \xi_6 = \lambda_3 = 0$. Using the obtained system of equations, we get the reduced system of equations. By solving the reduced system of equations using Maple we get the values of parameters:

$$\begin{aligned} \xi_2 &= \frac{\xi_3 \lambda_1}{3\lambda_2}, \quad \xi_3 = \xi_3, \quad \xi_4 = \frac{3\xi_5 \xi_8 \lambda_2^2}{\xi_3 \lambda_1^2}, \quad \xi_5 = \xi_5, \quad \xi_7 = 0, \\ \xi_8 &= \xi_8, \quad n_0 = n_0, \quad \xi_3 = \xi_3, \quad \lambda_1 = \lambda_1, \quad \lambda_2 = \lambda_2, \\ \xi_9 &= \frac{-9\beta \xi_3^2 \xi_8^2 \lambda_1^4 \lambda_2^4 - 81\beta \xi_5^2 \xi_8^2 \lambda_2^8 + 2\beta \xi_3^4 \lambda_1^6 - 54\xi_3^2 \xi_8^2 \lambda_1^2 \lambda_2^4}{9\beta \xi_3^2 \lambda_1^4 \lambda_2^4}. \end{aligned}$$

Using the derived parametric values in Eq. (13) along with Eq. (2), we get periodic solution for Eq. (1).

$$\begin{aligned} \Omega(x, y, t) &= m_0 + 2\beta \left(\frac{2\xi_5 \xi_8 \lambda_2}{\lambda_1} + \frac{\xi_3^2 (2y \lambda_1^2 \lambda_2^2 + 6t \lambda_1 \lambda_2^3)}{9\lambda_2^4} - n_0 \lambda_2 \sin(x \lambda_1 + y \lambda_2) \right) \\ &\times \left(\frac{-6\xi_8^2}{\beta \lambda_1^2} + \frac{\xi_3^2 (6ty \lambda_1 \lambda_2^3 + 9t^2 \lambda_2^4 + \lambda_1^2 (2 + y^2 \lambda_2^2))}{9\lambda_2^4} \right. \\ &\left. + \xi_5 \left(\xi_5 x^2 + 2\xi_8 \left(x + \frac{\lambda_2 (y \lambda_1 + 3t \lambda_2)}{\lambda_1^2} \right) + n_0 \cos(x \lambda_1 + y \lambda_2) \right) \right)^{-1}, \tag{14} \end{aligned}$$

where Ω represents the periodic solution of Eq. (1).

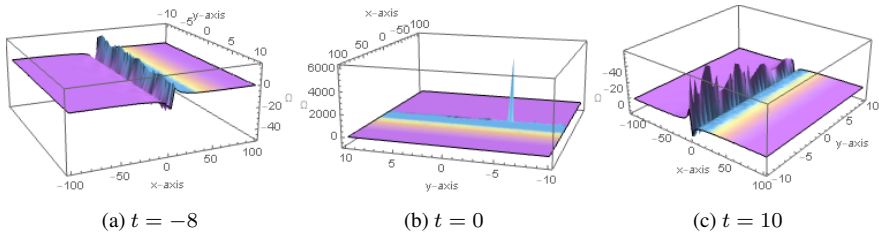


Figure 13. The 3-D plots for $\Omega(x, y, t)$ in Eq. (14) are presented with the following values of parameters: $\lambda_1 = 10, \lambda_2 = 2, n_0 = 20, \xi_3 = 4, \xi_8 = 5, \xi_5 = 0.7, m_0 = -0.5, \beta = 9$ in interval $-100 \leq x \leq 100$ and $-10 \leq y \leq 10$.

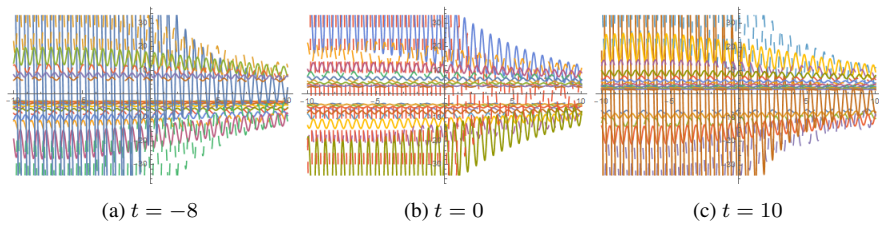


Figure 14. The 2-D plots for $\Omega(x, y, t)$ in Eq. (14) are presented with the following parametric values: $\lambda_1 = 10, \lambda_2 = 2, n_0 = 20, \xi_3 = 4, \xi_8 = 5, \xi_5 = 0.7, m_0 = -0.5, \beta = 9$.

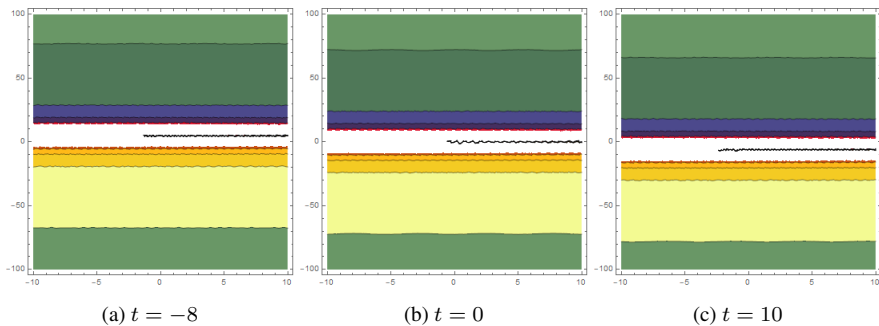


Figure 15. The contour plots for $\Omega(x, y, t)$ in Eq. (14) are presented with the following values of parameters: $\lambda_1 = 10, \lambda_2 = 2, n_0 = 20, \xi_3 = 4, \xi_8 = 5, \xi_5 = 0.7, m_0 = -0.5, \beta = 9$ in interval $-100 \leq x \leq 100$ and $-10 \leq y \leq 10$.

6.2 Set-II

We consider $\xi_1 = \xi_6 = \lambda_3 = 0$. Using the obtained system of equations, we get the reduced system of equations. By solving reduced system of equations using Maple we get the values of parameters:

$$\xi_1 = \xi_6 = \lambda_3 = 0, \quad \xi_2 = 0, \quad \xi_3 = i\xi_7,$$

$$\xi_4 = \frac{-i\xi_8(\beta\xi_5\lambda_2^2 - \lambda_7)}{\xi_7}, \quad \xi_5 = \xi_5, \quad \lambda_2 = \lambda_2, \quad \xi_7 = \xi_7, \quad \xi_8 = \xi_8,$$

$$\xi_9 = \frac{\beta\xi_5\lambda_2^2\xi_8^2(\beta\xi_5\lambda_2^2 - 2\xi_7)}{\xi_7^2}, \quad n_0 = n_0, \quad \lambda_1 = \lambda_1.$$

With the help of obtained parametric values in Eq. (13) along with Eq. (2), we find periodic solution for Eq. (1).

$$\begin{aligned} \Omega(x, y, t) = & m_0 - 2\beta n_0 \lambda_2 \sin(x\lambda_1 + y\lambda_2) \\ & \times \left((\xi_8 + \xi_7 t + \xi_5 x)^2 + \frac{\beta\xi_5\xi_8^2\lambda_2^2(-2\xi_7 + \beta\xi_5\lambda_2^2)}{\xi_7^2} \right. \\ & \left. + \left(i\xi_7 t - \frac{i\xi_8(-\xi_7 + \beta\xi_5\lambda_2^2)}{\xi_7} \right)^2 + n_0 \cos(x\lambda_1 + y\lambda_2) \right)^{-1}, \end{aligned}$$

where Ω specify the periodic solution of Eq. (1).

7 Multi-waves

For multiwaves, we use given transformation [29]

$$\rho = \psi_1 \cosh(\phi_1) + \psi_2 \cos(\phi_2) + \psi_3 \cosh(\phi_3) + \rho_0, \tag{15}$$

where

$$\begin{aligned} \psi_1 = \xi_1 x + \xi_2 y + \xi_3 t + \xi_4, \quad \psi_2 = \xi_5 x + \xi_6 y + \xi_7 t + \xi_8, \\ \psi_3 = \xi_9 x + \xi_{10} y + \xi_{11} t + \xi_{12}. \end{aligned}$$

However, ξ_α ($1 \leq \alpha \leq 12$) are real valued parameters, which we will find. Now we insert Eq. (15) into Eq. (3) and we identify the coefficients of x, y, t and trigonometric functions to be zero. We gather system of equations after resolving the system of equations in Maple. We collect different values of involved parameters.

7.1 Set-I

We assume $\xi_1 = \xi_6 = 0$. Then with the help of assumed parameters, we get remaining values:

$$\begin{aligned} \xi_1 = 0, \quad \xi_6 = 0, \quad \xi_{10} = \frac{1}{6}, \quad \xi_{11} = \xi_{11}, \quad \xi_{12} = \xi_{12}, \quad \xi_3 = \frac{(108\xi_2^2 + 1)\sqrt{36}}{216\sqrt{1/\beta}}, \\ \xi_4 = \xi_4, \quad \xi_5 = \xi_5, \quad \xi_7 = \xi_7, \quad \xi_8 = \xi_8, \quad \xi_2 = \xi_2, \quad \xi_9 = \frac{\sqrt{36}\sqrt{1/\beta}}{36\xi_2}. \end{aligned}$$

Using the above parametric values in Eq. (15), then in Eq. (2), we get multiwave solution for Eq. (1).

$$\begin{aligned} \Omega(x, y, t) = & m_0 + 2\beta \left(\frac{1}{6} \psi_3 \sinh \left(\xi_{12} + \xi_{11} t + \xi_9 x + \frac{y}{6} \right) \right. \\ & \left. + \sqrt{\frac{1}{\beta}} \psi_1 \sinh \left(\xi_4 + \frac{\sqrt{\frac{1}{\beta}}(3 + \xi_9^2 \beta)t}{36\xi_2^2} + \sqrt{\frac{1}{\beta}} y \right) \right) \end{aligned}$$

$$\begin{aligned} & \times \left(\rho_0 + \psi \cosh \left(\xi_{12} + \xi_{11}t + \xi_9x + \frac{y}{6} \right) \right. \\ & \left. + \psi_1 \cosh \left(\xi_4 + \frac{\sqrt{\frac{1}{\beta}}(3 + \xi_9^2\beta)t}{36\xi_9^2} + \frac{\sqrt{\frac{1}{\beta}}y}{6\xi_9} \right) \right)^{-1}, \end{aligned} \tag{16}$$

where Ω represents the multiwave solution of Eq. (1).

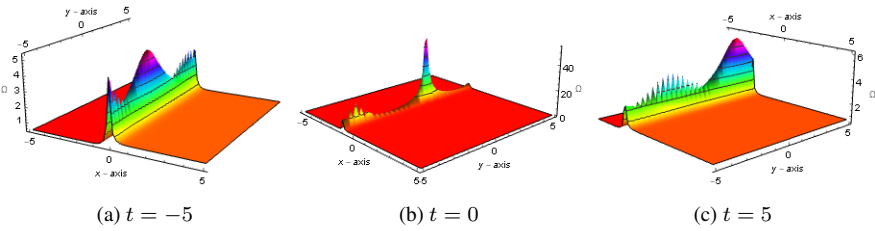


Figure 16. The 3-D plots for $\Omega(x, y, t)$ in Eq. (16) are presented with the following values of parameters: $\psi_3 = 28, \rho_0 = -8, \psi_1 = -4, \xi_9 = 5, \xi_{11} = 1, \xi_4 = 20, \xi_2 = -1, \xi_{12} = 25, m_0 = 0.5, \beta = -3.9$ in interval $-5 \leq x, y \leq 5$.

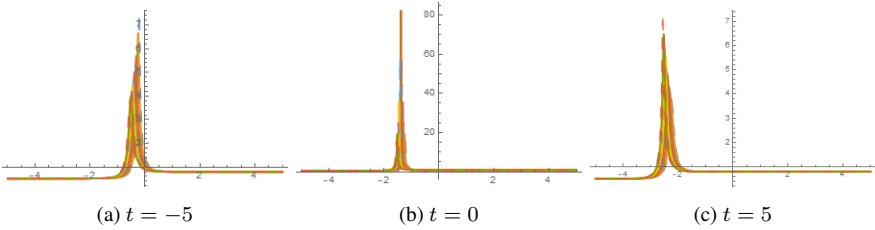


Figure 17. The 2-D plots for $\Omega(x, y, t)$ in Eq. (16) are presented with the following parametric values: $\psi_3 = 28, \rho_0 = -8, \psi_1 = -4, \xi_9 = 5, \xi_{11} = 1, \xi_4 = 20, \xi_2 = -1, \xi_{12} = 25, m_0 = 0.5, \beta = -3.9$.

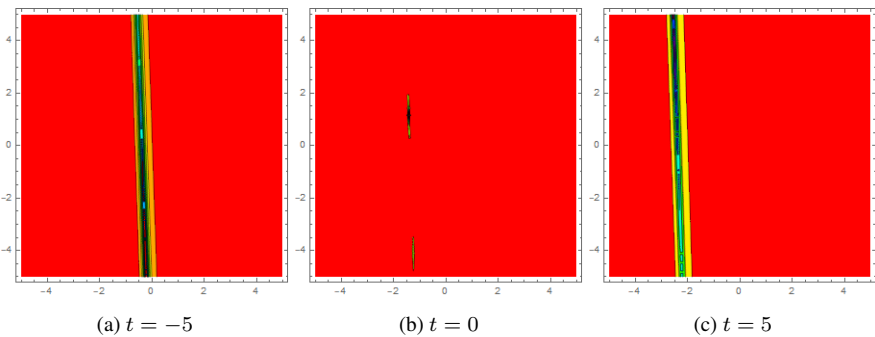


Figure 18. The contour plots for $\Omega(x, y, t)$ in Eq. (16) are presented with the following values of parameters: $\psi_3 = 28, \rho_0 = -8, \psi_1 = -4, \xi_9 = 5, \xi_{11} = 1, \xi_4 = 20, \xi_2 = -1, \xi_{12} = 25, m_0 = 0.5, \beta = -3.9$ in interval $-5 \leq x, y \leq 5$.

7.2 Set-II

We consider $\xi_1 = \xi_6 = 0$. By using these parametric values we get values of other parameters:

$$\begin{aligned} \xi_{10} &= \frac{1}{6}, \quad \xi_{11} = \xi_{11}, \quad \xi_{12} = \xi_{12}, \quad \xi_2 = 6\sqrt{3}\sqrt{\frac{36\xi_3\sqrt{\beta} + \beta}{\beta(1296\xi_3^2 - b)}} \frac{\xi_3}{\frac{36\xi_3\sqrt{\beta} + \beta}{\beta(1296\xi_3^2 - \beta) + 3}}, \\ \xi_3 &= \xi_3, \quad \xi_4 = \xi_4, \quad \xi_5 = \xi_5, \quad \xi_7 = \xi_7, \quad \xi_8 = \xi_8, \\ \xi_9 &= \sqrt{3}\sqrt{\frac{36\xi_3\sqrt{\beta} + \beta}{\beta(1296\xi_3^2 - \beta)}}, \quad \psi_1 = \psi_1, \quad \psi_2 = 0, \quad \psi_3 = \psi_3. \end{aligned}$$

Using derived parametric values in Eq. (15) along with Eq. (2), we get multiwave solution for Eq. (1).

$$\begin{aligned} \Omega(x, y, t) &= m_0 + 2\beta \left(\frac{1}{6}\psi_3 \sinh \left(\xi_{12} + \xi_{11}t + \sqrt{3}\sqrt{\frac{36\xi_3\sqrt{\beta} + \beta}{(1296\xi_3^2 - \beta)\beta}}x + \frac{y}{6} \right) \right. \\ &\quad \left. + \frac{6\sqrt{3}\sqrt{\frac{36\xi_3\sqrt{\beta} + \beta}{(1296\xi_3^2 - \beta)\beta}}\psi_1 \sinh(\xi_4 + \xi_3t + 6\sqrt{3}\sqrt{\frac{36\xi_3\sqrt{\beta} + \beta}{(1296\xi_3^2 - \beta)\beta}}y)}{3 + \frac{3(36\xi_3\sqrt{\beta} + \beta)}{1296\xi_3^2 - \beta}} \right) \\ &\quad \times \left(\rho_0 + \psi_3 \cosh \left(\xi_{12} + \xi_{11}t + \sqrt{3}\sqrt{\frac{36\xi_3\sqrt{\beta} + \beta}{(1296\xi_3^2 - \beta)\beta}}x + \frac{y}{6} \right) \right. \\ &\quad \left. + \psi_1 \cosh \left(\xi_4 + \xi_3t + \frac{6\sqrt{3}\sqrt{\frac{36\xi_3\sqrt{\beta} + \beta}{(1296\xi_3^2 - \beta)\beta}}y}{3 + \frac{3(36\xi_3\sqrt{\beta} + \beta)}{1296\xi_3^2 - \beta}} \right) \right)^{-1}, \end{aligned}$$

where Ω indicates the multiwave solution of Eq.(1).

8 Interaction between lump, periodic and lump with I-kink

We use bilinear form given in Eq. (3) along with following transformation [28]:

$$\rho = \phi^2 + \psi^2 + \xi_9 + b_1 \cos(\lambda_1x + \lambda_2y + \lambda_3t) + b_2e^{\lambda_4x + \lambda_5y + \lambda_6t}, \tag{17}$$

where

$$\phi = \xi_1x + \xi_2y + \xi_3t + \xi_4, \quad \psi^2 = \xi_5x + \xi_6y + \xi_7t + \xi_8.$$

However, ξ_α ($1 \leq \alpha \leq 9$) and λ_α ($1 \leq \alpha \leq 6$) are real valued parameters, which we will find. Now we insert Eq. (17) into Eq. (3) and identify the coefficients of x, y, t , exponential function and trigonometric functions to be zero. We gather system of equations after resolving the system of equations in Maple, we collect different values of parameters involved.

8.1 Set-I

We assume that $\xi_1 = \xi_7 = \xi_8 = \lambda_2 = 0$. Then with the help of assumed parameters, we get other values:

$$\begin{aligned} \lambda_1 &= \lambda_1, \quad \lambda_3 = 0, \quad \lambda_4 = \lambda_4, \quad \xi_2 = I\xi_6, \\ \xi_3 &= \frac{-2I\xi_6(\beta\lambda_4 + \lambda_5^2 + \lambda_6)}{\lambda_5}, \quad \xi_9 = \xi_9, \\ b_2 &= b_2, \quad \xi_4 = 0, \quad b_1 = b_1, \quad \xi_6 = \xi_6, \\ \xi_5 &= \frac{2\xi_6(\beta\lambda_1^2\lambda_5^2 + \beta\lambda_4^2\beta_5^2 - \lambda_4^2\lambda_6^2 + \lambda_4\lambda_6 + 3\lambda_5^2)}{\lambda_5 + \lambda_6}. \end{aligned}$$

Using the above parametric values in Eq. (17) with Eq. (2), we get multiwave solution for Eq. (1).

$$\begin{aligned} \Omega(x, y, t) &= m_0 + 2\beta \left(\lambda_5 e^{\lambda_6 t + \lambda_4 x + \lambda_5 y} b_2 + 2i\xi_6 \left(\frac{-2i(\beta\lambda_4\lambda_5^2 + \lambda_6)\xi_6 t}{\lambda_5} + i\xi_6 y \right) \right. \\ &\quad \left. + \frac{2(3\lambda_5^2 + \beta\lambda_1^2\lambda_5^2 + \beta\lambda_4^2\lambda_5^2 + \lambda_4\lambda_6 - \lambda_4^2\lambda_6^2)\xi_6 x}{\lambda_5\lambda_6} + \xi_6 y \right) \\ &\quad \times \left(\xi_9 + e^{\lambda_6 t + \lambda_4 x + \lambda_5 y} b_2 \left(\frac{-2i(\beta\lambda_4\lambda_5^2 + \lambda_6)\xi_6 t}{\lambda_5} + i\xi_6 y \right)^2 \right. \\ &\quad \left. + \frac{2(3\lambda_5^2 + \beta\lambda_1^2\lambda_5^2 + \beta\lambda_4^2\lambda_5^2 + \lambda_4\lambda_6 - \lambda_4^2\lambda_6^2)\xi_6 x}{\lambda_5\lambda_6} + \xi_6 \right. \\ &\quad \left. + b_1 \cos(\lambda_1 x) \right)^{-1}, \end{aligned} \tag{18}$$

where Ω indicates the interaction between lump, periodic and lump with I-kink solution of Eq. (1).

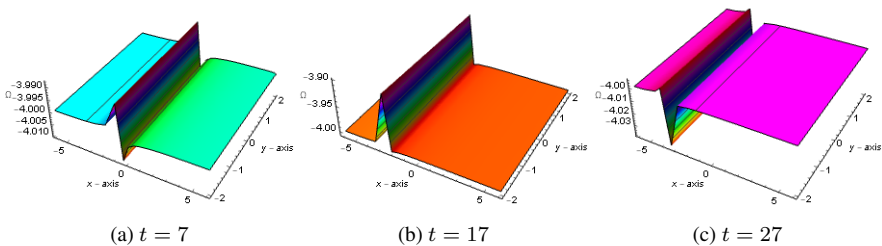


Figure 19. The 3-D plots for $\Omega(x, y, t)$ in Eq. (18) are presented with the following values of parameters: $\lambda_6 = -8, \lambda_4 = 8, \lambda_5 = 10, \lambda_1 = -25, \lambda_2 = 20, \xi_6 = -5, \xi_9 = 1, b_1 = 7, b_2 = -1, m_0 = -4, \beta = 3$ in interval $-5 \leq x \leq 5$ and $-2 \leq y \leq 2$.

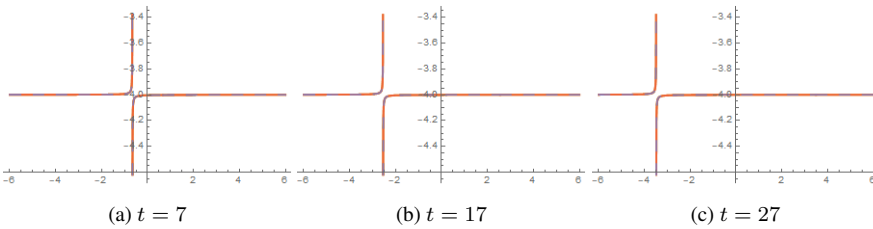


Figure 20. The 2-D plots for $\Omega(x, y, t)$ in Eq. (18) are presented with the following parametric values: $\lambda_6 = -8, \lambda_4 = 8, \lambda_5 = 10, \lambda_1 = -25, \lambda_2 = 20, \xi_6 = -5, \xi_9 = 1, b_1 = 7, b_2 = -1, m_0 = -4, \beta = 3$.

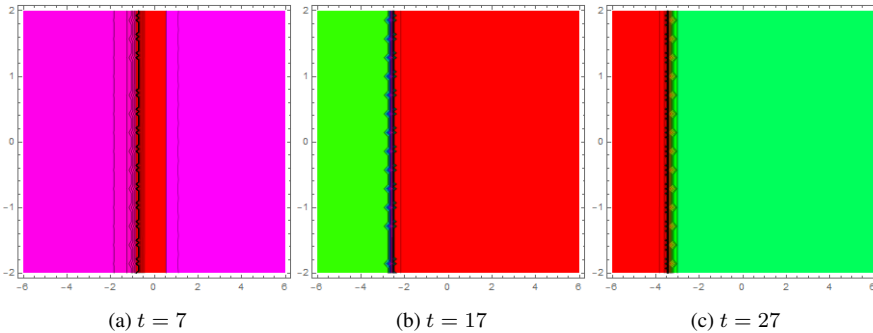


Figure 21. The contour plots for $\Omega(x, y, t)$ in Eq. (18) are presented with the following values of parameters: $\lambda_6 = -8, \lambda_4 = 8, \lambda_5 = 10, \lambda_1 = -25, \lambda_2 = 20, \xi_6 = -5, \xi_9 = 1, b_1 = 7, b_2 = -1, m_0 = -4, \beta = 3$ in interval $-5 \leq x \leq 5$ and $-2 \leq y \leq 2$.

8.2 Set-II

We consider $\xi_1 = \xi_7 = \xi_8 = \lambda_2 = 0$. Using assumed parametric values and using the obtained system of equations, we get reduced system of equations. By solving reduced system of equations using Maple we get the values of parameters:

$$\lambda_1 = \sqrt{\frac{(-\lambda_5(\beta^2\lambda_4^3\lambda_5^4 - \beta\lambda_4^3\lambda_5^2\lambda_6^2 + 2\beta\lambda_4^2\lambda_5^2\lambda_6^2 + 3\beta\lambda_4\lambda_5^4 - \lambda_4^2\lambda_6^3 + \lambda_4\lambda_6^2 + 3\lambda_5^2\lambda_6))}{\beta\lambda_4\lambda_5^2 + 2\beta\lambda_6}},$$

$$\lambda_3 = 0, \quad \lambda_4 = \lambda_4, \quad \xi_2 = \xi_2,$$

$$\xi_3 = \frac{-2\xi_2(\beta\lambda_4\lambda_5^2 + \lambda_6)}{\lambda_5}, \quad \xi_4 = 0, \quad \xi_5 = \frac{2(\beta\lambda_4^2\lambda_5^2 - \lambda_4^2\lambda_6^2 + \lambda_4\lambda_6 + 3\lambda_5^2)\xi_6}{(\beta\lambda_4\lambda_5^2 + 2\lambda_6)\lambda_5},$$

$$\xi_6 = \xi_6, \quad \xi_9 = \xi_9, \quad b_1 = b_1, \quad b_2 = b_2.$$

Using the above parametric values in Eq. (17) along with Eq. (2), we get multiwave solution for Eq. (1).

$$\Omega(x, y, t) = m_0 + 2\beta \left(\lambda_5 e^{\lambda_6 t + \lambda_4 x + \lambda_5 y} m_2 + 2\xi_2 \frac{-2(\beta\lambda_4\lambda_5^2 + \lambda_6)\xi_2 t}{\lambda_5} + \xi_3 y \right)$$

$$\begin{aligned}
 &+ 2\xi_6 \left(\frac{2(3\lambda_5^2 + \beta\lambda_4^2\lambda_5^2 + \lambda_4\lambda_6 - \lambda_4^2\lambda_6^2)\xi_6x}{\lambda_5(\beta\lambda_4\lambda_5^2 + 2\lambda_6)} + \xi_6y \right) \\
 &\times \left(\xi_9 + e^{\lambda_6t + \lambda_4x + \lambda_5y} m_2 + \left(\frac{-2(\beta\lambda_4\lambda_5^2 + \lambda_6)\xi_2t}{\lambda_5} + \xi_3y \right)^2 \right. \\
 &\left. + \left(\frac{2(3\lambda_5^2 + \beta\lambda_4^2\lambda_5^2 + \lambda_4\lambda_6 - \lambda_4^2\lambda_6^2)\xi_6x}{\lambda_5(\beta\lambda_4\lambda_5^2 + 2\lambda_6)} + \xi_6y \right)^2 + m_1 \cos \mathfrak{C} \right)^{-1},
 \end{aligned}$$

where

$$\mathfrak{C} = \sqrt{\frac{-3\beta\lambda_4\lambda_5^4 - \beta^2\lambda_4^3\lambda_5^4 - 3\lambda_5^2\lambda_6 - 2\beta\lambda_4^2\lambda_5^2\lambda_6 - \lambda_4\lambda_6^2 + \beta\lambda_4^3\lambda_5^2\lambda_6^2 + \lambda_4^2\lambda_6^3}{\lambda_5(\beta^2\lambda_4\lambda_5^2 + 2\beta\lambda_6)}},$$

and Ω represents the interaction between lump, periodic and lump with I-kink solution of Eq. (1).

9 Results and discussions

A comprehensive comparison between earlier literature with our accomplished outcomes is discussed in this section. Several researchers worked on various techniques for computing soliton solutions for our governing model. Particularly, Pavlov [26] constructed Benny-type moment chains, Santini [25] presented inverse scattering problem for Pavlov equation, Baran et al. [5] derived symmetry reduction, Grinevich [12] et al. worked on cauchy problem for Pavlov equation, Baran et al [6] applied Lax representation to symmetry reductions, Wu [33] utilized Newtonian iteration approach. Moreover, Morozov [16] used conservation laws. Here in this presented work, we computed the lump solution, lump with I-kink, lump with II-kink, periodic solution, multiwave, rogue wave, interaction between lump and periodic and lump with I-kink for Pavlov equation using ansatz transformation.

These solutions have significant importance in various fields of sciences for instance, chemistry biology, mathematical physics, oceanographic engineering, capillary flow, finance and nonlinear optics. To demonstrate the variety of obtained solutions distinctly, different parametric values are used. The desired solutions have been presented graphically via 3-D and contour plots, and we observe how our derived results reshape with arbitrary values of t . In Fig. 1(a), we can see that Ω is maximum at some point, Fig. 1(b) presents 3-D plots of Ω discussing bright dark lump, Fig. 1(c) shows the corresponding contour plots for lump solution. Figure 4 shows lump with I-kink when $t = -10, t = 0$ and $t = 10$. Contour plots of lump with I-link are presented in Fig. 6. In Fig. 7, we can clearly see lump with II-kink wave. In case of rogue wave when $t = -2$, Fig. 10(a) shows two bright lumps. When t increases, lump waves steadily come closer to each other, and after interaction, they become a single stilton. Contour plots of the rogue wave shown in Fig. 12. Figure 13 shows the periodic wave for solution Eq. (14). In Fig. 16, 3-D plot of multiwave solution for Eq. (16) presented with arbitrary values of t . Figure 19 shows bright dark lump, Figs. 19(b) and 19(c) show bright and dark lumps, respectively.

10 Conclusion

The motivation of the presented article is to cumulate the lump solutions, lump with I-kink, lump with II- kink, periodic solutions, multiwave, rogue wave, interaction between lump periodic and I-kink and interaction between lump for Pavlov equation by ansatz transformation and through explaining applicable transformations. We have fortunately produced some modish exact solutions for the related model. The 3-D and contour graphs plotted with the distinct numeric values to examine the physical response of the system. For finer understanding and consideration we have also discussed the geometry of the graphs. The achieved solutions exhibit that the suggested method is well founded, definitive and straightforward. Therefore, the proposed scheme could be expanded for advanced nonlinear models in mathematical physics.

References

1. M.A. Ablowitz, P.A. Clarkson, *Solitons Nonlinear Evolution Equations and Inverse Scattering*, Lond. Math. Soc. Lect. Note Ser., Vol. 149, Cambridge Univ. Press, Cambridge, 1991, <https://doi.org/10.1017/CBO9780511623998>.
2. G.P. Agrawal, *Nonlinear Fiber Optics*, 2nd ed., 592, Academic Press, San Diego, CA, 1995, <https://doi.org/10.1016/C2009-0-21165-2>.
3. I. Ahmed, A.R. Seadawy, D. Lu, Kinky breathers, W-shaped and multi-peak solitons interaction in (2+1)-dimensional nonlinear Schrödinger equation with Kerr law of nonlinearity, *Eur. Phys. J. Plus*, **134**:120, 2019, <https://doi.org/10.1140/epjp/i2019-12482-8>.
4. I. Ahmed, A.R. Seadawy, D. Lu, M-shaped rational solitons and their interaction with kink waves in the Fokas–Lenells equation, *Phys Scr.*, **94**(5):055205, 2019, <https://doi.org/10.1088/1402-4896/ab0455>.
5. H. Baran, I.S. Krasichik, O.I. Morozov, Symmetry reductions and exact solutions of Lax integrable 3-dimensional systems, *J. Nonlinear Math. Phys.*, **21**(4):643–671, 2014, <https://doi.org/10.1080/14029251.2014.975532>.
6. H. Baran, I.S. Krasichik, O.I. Morozov, Integrability properties of some equations obtained by symmetry reductions, *J. Nonlinear Math. Phys.*, **22**(2):210–232, 2015, <https://doi.org/10.1080/14029251.2015.1023582>.
7. T. Batool, S.T.R. Rizvi, A.R. Seadawy, Multiple breathers and rational solutions to Ito integro-differential equation arising in shallow water waves, *J. Geom. Phys.*, **178**:104540, 2022, <https://doi.org/10.1016/j.geomphys.2022.104540>.
8. N. Benoudina, Y. Zhang, C.M. Khalique, Lie symmetry analysis, optimal system, new solitary wave solutions and conservation laws of the Pavlov equation, *Commun. Nonlinear Sci. Numer. Simul.*, **94**:105560, 2021, <https://doi.org/10.1016/j.cnsns.2020.105560>.
9. N. Celik, A.R. Seadawy, Y.S. Ozkan, E. Yasar, A model of solitary waves in a nonlinear elastic circular rod: Abundant different type exact solutions and conservation laws, *Chaos Solitons Fractals*, **143**:110486, 2021, <https://doi.org/10.1016/j.chaos.2020.110486>.

10. M.K. Elboree, The Jacobi elliptic function method and its application for two component BKP hierarchy equations, *Comput. Math. Appl.*, **62**:4402–4414, 2011, <https://doi.org/10.1016/j.camwa.2011.10.015>.
11. O.F. Gözükcı, S. Akçağıl, The tanh-coth method for some nonlinear pseudoparabolic equations with exact solutions, *Adv. Difference Equ.*, **2013**:143, 2013, <https://doi.org/10.1186/1687-1847-2013-143>.
12. G. Grinevich, P.M. Santini, D. Wu, The Cauchy problem for the Pavlov equation, *Nonlinearity*, **28**(11):3709, 2015, <https://doi.org/10.1088/0951-7715/28/11/3709>.
13. B. Guo, H. Dong, Y. Fang, Lump solutions and interaction solutions for the dimensionally reduced nonlinear evolution equation, *Complexity*, **2019**:5765061, 2019, <https://doi.org/10.1155/2019/5765061>.
14. K. Imai, K. Nozaki, Lump solutions of the Ishimori-II equation, *Prog. Theor. Phys.*, **96**(3):521–526, 1996, <https://doi.org/10.1143/PTP.96.521>.
15. S. Kumar, M. Kumar, D. Kumar, Computational soliton solutions to $(2 + 1)$ -dimensional Pavlov equation using Lie symmetry approach, *Pramana – J. Phys.*, **94**:28, 2020, <https://doi.org/10.1007/s12043-019-1894-0>.
16. A. Lelito, O.I. Morozov, Three-component nonlocal conservation laws for Lax-integrable 3D partial differential equations, *J. Geom. Phys.*, **131**:89–100, 2018, <https://doi.org/10.1016/j.geomphys.2018.05.004>.
17. J.G. Liu, Lump-type solutions and interaction solutions for the $(2+1)$ -dimensional generalized fifth-order KdV equation, *Appl. Math. Lett.*, **86**:36–41, 2018, <https://doi.org/10.1016/j.aml.2018.06.011>.
18. W.-X. Ma, Nonlocal integrable mKdV equations by two nonlocal reductions and their soliton solutions, *J. Geom. Phys.*, **177**:104522, 2022, <https://doi.org/10.1016/j.geomphys.2022.104522>.
19. W.-X. Ma, Riemann–Hilbert problems and inverse scattering of nonlocal real reverse-spacetime matrix AKNS hierarchies, *Physica D*, **430**:133078, 2022, <https://doi.org/10.1016/j.physd.2021.133078>.
20. W.-X. Ma, Riemann–Hilbert problems and soliton solutions of nonlocal reverse-time NLS hierarchies, *Acta Math. Sci.*, **42**:127–140, 2022, <https://doi.org/10.1007/s10473-022-0106-z>.
21. W.-X. Ma, Riemann–Hilbert problems and soliton Solutions of type $(\lambda, -\lambda^*)$ reduced nonlocal integrable mKdV hierarchies, *Mathematics*, **10**(6):870, 2022, <https://doi.org/10.3390/math10060870>.
22. W.-X. Ma, Type $(-\lambda, -\lambda^*)$ reduced nonlocal integrable mKdV equations and their soliton solutions, *Appl. Math. Lett.*, **131**:108074, 2022, <https://doi.org/10.1016/j.aml.2022.108074>.
23. W.X. Ma, Lump solutions to the Kadomtsev–Petviashvili equation, *Phys. Lett. A*, **379**(36):1975–1978, 2015, <https://doi.org/10.1016/j.physleta.2015.06.061>.
24. W.X. Ma, Y. Zhou, Lump solutions to nonlinear partial differential equations via Hirota bilinear forms, *J. Differ. Equations*, **264**:2633–2659, 2018, <https://doi.org/10.1016/j.jde.2017.10.033>.

25. S.V. Manakov, P.M. Santini, On the solutions of the second heavenly and Pavlov equations, *J. Phys. A, Math. Theor.*, **42**:404013, 2009, <https://doi.org/10.1088/1751-8113/42/40/404013>.
26. M.V. Pavlov, Integrable hydrodynamic chains, *J. Math. Phys.*, **44**:4134, 2003, <https://doi.org/10.1063/1.1597946>.
27. N. Raza, A.R. Seadawy, M. Kaplan, A.R. Butt, Symbolic computation and sensitivity analysis of nonlinear Kudryashov's dynamical equation with applications, *Phys Scr.*, **96**:105216, 2021, <https://doi.org/10.1088/1402-4896/ac0f93>.
28. B. Ren, J. Lin, Z.M. Lou, A new nonlinear equation with lump-Soliton, lump periodic, and lump periodic soliton solutions, *Complexity*, **2019**:4072754, 2019, <https://doi.org/10.1155/2019/4072754>.
29. S.T.R. Rizvi, A.R. Seadawy, T. Batool, M.A. Ashraf, Homoclinic breathers, multivariate, periodic cross-kink and periodic cross-rational solutions for improved perturbed nonlinear Schrödinger's with quadratic-cubic nonlinearity, *Chaos Solitons Fractals*, **161**:112353, 2022, <https://doi.org/10.1016/j.chaos.2022.112353>.
30. A.R. Seadawy, H.M. Ahmed, W.B. Rabie, A. Biswas, An alternate pathway to solitons in magneto-optic waveguides with triple-power law nonlinearity, *Optik*, **231**:166480, 2021, <https://doi.org/10.1016/j.ijleo.2021.166480>.
31. A.R. Seadawy, K. El-Rashidy, Application of the extension exponential rational function method for higher-dimensional Broer–Kaup–Kupershmidt dynamical system, *Mod. Phys. Lett. A*, **35**(1):1950345, 2020, <https://doi.org/10.1142/S0217732319503450>.
32. B.H. Wang, P.H. Lu, C.Q. Dai, Y.X. Chen, Vector optical soliton and periodic solutions of a coupled fractional nonlinear Schrödinger equation, *Results Phys.*, **17**:103036, 2020, <https://doi.org/10.1016/j.rinp.2020.103036>.
33. D. Wu, The Cauchy problem for the Pavlov equation with large data, *J. Differ. Equations*, **263**(3):1874–1906, 2017, <https://doi.org/10.1016/j.jde.2017.03.033>.
34. X.W. Yan, S.F. Tian, M.J. Dong, Backlund transformation, rogue wave solutions and interaction phenomena for a $(3 + 1)$ -dimensional B-type Kadomtsev–Petviashvili–Boussinesq equation, *Nonlinear Dyn.*, **92**(2):709–720, 2018, <https://doi.org/10.1007/s11071-018-4085-5>.
35. H. Yilmaz, Exact solutions of the Gerdjikov–Ivanov equation using Darboux transformations, *J. Nonlinear Math. Phys.*, **22**:32–46, 2015, <https://doi.org/10.1080/14029251.2015.996438>.
36. U. Younas, M. Younis, A.R. Seadawy, S.T.R. Rizvi, S. Althobaiti, S. Sayed, Diverse exact solutions for modified nonlinear Schrödinger equation with conformable fractional derivative, *Results Phys.*, **20**:103766, 2021, <https://doi.org/10.1016/j.rinp.2020.103766>.
37. J.B. Zhang, W.X. Ma, Mixed lump-kink solutions to the BKP equation, *Comput. Math. Appl.*, **74**:591–596, 2017, <https://doi.org/10.1016/j.camwa.2017.05.010>.
38. X. Zhang, Y. Chen, Rogue wave and a pair of resonance stripe solitons to a reduced $(3 + 1)$ -dimensional Jimbo–Miwa equation, *Commun. Nonlinear Sci. Numer. Simul.*, **52**:24–31, 2017, <https://doi.org/10.1016/j.cnsns.2017.03.021>.

39. Z. Zhao, Y. Chen, B. Han, Lump soliton, mixed lump stripe and periodic lump solutions of a $(2 + 1)$ -dimensional asymmetrical Nizhnik–Novikov–Veselov equation, *Mod. Phys. Lett. B*, **31**:1750157, 2017, <https://doi.org/10.1142/S0217984917501573>.
40. Y. Zhou, S. Manukure, W. Ma, Lump and lump-soliton solutions to the Hirota–Satsuma–Ito equation, *Commun. Nonlinear Sci. Numer. Simul.*, **68**:56–62, 2019, <https://doi.org/10.1016/j.cnsns.2018.07.038>.